Data in Brief 52 (2024) 109862

Contents lists available at ScienceDirect

Data in Brief

journal homepage: www.elsevier.com/locate/dib

Data Article

Fatigue dataset of hybrid non-toughened and toughened epoxy adhesives

Dharun Vadugappatty Srinivasan, Anastasios P. Vassilopoulos*

Composite Construction Laboratory (CCLab), Station 16, Ecole Polytechnique Fédérale de Lausanne (EPFL), Lausanne CH-1015, Switzerland

A R T I C L E I N F O

Article history:
Received 23 August 2023
Revised 10 October 2023
Accepted 22 November 2023
Available online 28 November 2023

Dataset link: Fatigue dataset of hybrid non-toughened and toughened epoxy adhesives (Original data)

Keywords:
Fatigue
Composites
Adhesives
Toughening
Geometry effect
Failure analysis
Wind turbine rotor blades

A B S T R A C T

In this article, four different structural epoxy adhesives such as SPABOND™ 820HTA (non-toughened), SPABOND™ 840HTA (toughened) adhesives, and their two hybrid combinations are fabricated using a manual mixing method. Quasi-static tensile experiments are conducted at standardized and high strain rates using ASTM D638-22 Type II specimens to investigate the strain rate effects on the tensile properties. Tensile-tensile fatigue experiments are performed using ASTM D638-22 Type I and Type II specimens to evaluate the impact of specimen geometry and toughening on fatigue life. The digital image correlation technique is utilized to obtain full-field strain data in these experiments. Technical data analysis, plotting, smoothing, filtering, and averaging are carried out using Origin Pro® and MATLAB R2021b®. The obtained S-N curve data can be used to develop fatigue failure criteria and predict the behavior of wind turbine blade adhesive joints through finite element modeling.

DOI of original article: 10.1016/j.polymertesting.2023.107975

* Corresponding author.
E-mail address: anastasios.vassilopoulos@epfl.ch (A.P. Vassilopoulos).

https://doi.org/10.1016/j.dib.2023.109862

Specifications Table

Subject	Materials science: Polymers and plastics
Specific subject area	Quasi-static tensile and fatigue life of epoxy adhesives
Type of data	Table Figure
How the data were acquired	Different experiments were carried out and the corresponding data were acquired as follows: • Quasi-static tensile and tensile-tensile fatigue experiments using MTS® 810 Landmark servo-hydraulic machine with a calibrated load cell of 5 kN. • Quasi-static high strain-rate tensile experimental imaging for digital image correlation (DIC) using high-speed imaging camera FASTCAM SA- Z from Photron along with AF-S NIKKOR 50mm lens • Quasi-static standardized strain-rate tensile and fatigue experimental imaging for digital image correlation (DIC) using Point Grey – Grasshopper 3 camera (2.2 Megapixels) housing Fujinon HF35SA-1 35 mm F/1.4 lens. • Catman® data acquisition system (DAQ) for high strain-rate tensile testing • Digital image correlation using VIC 2D-6 software from correlated solutions® • An in-house developed LabVIEW® software for acquiring images and forces values from the test machine. • Sony XCG-5005E (5 Megapixels) camera with 2448 $\times$ 2048 pixels resolution. • Origin Pro® software for smoothing, filtering, and averaging the plots.
Data format	Raw Analyzed Filtered
Description of data collection	The engineering tensile stress and strain values of the specimens were obtained through DIC analysis. Based on these values, the true stress and strain were calculated and smoothed using Origin Pro® software. The tensile properties, including Young's modulus, ultimate strength, failure strain, and tensile toughness were determined using the MATLAB R2021b® software program. In the fatigue experiments, the cyclic strain was calculated through DIC analysis, and the corresponding cycle count and load were recorded by LabVIEW® software. The MATLAB R2021b® program was used to determine the hysteresis loops, cyclic stiffness, and mean strain from the measured cyclic stress and strain. Overall, Origin Pro® software was utilized for smoothing and filtering the plots.
Data source location	The Structural Engineering Platform, GIS-ENAC (https://www.epfl.ch/schools/enac/research/platforms-and-services/gis/), Composite Construction Laboratory (CCLab)/ Ecole Polytechnique Fédérale de Lausanne (EPFL), Lausanne, Switzerland.
Data accessibility	Repository name: Zenedo Data Data identification number: 10.5281/zenodo.7974626 Direct URL to data: https://zenodo.org/record/7974627
Related research article	D.V. Srinivasan, A.P. Vassilopoulos, Fatigue performance of wind turbine rotor blade epoxy adhesives, Polym Test. 121 (2023) 107975. https://doi.org/10.1016/J.POLYMERTESTING.2023.107975.

1. Value of the Data

- Data provides the static tensile stress-strain curves for different strain-rates of wind turbine blade adhesives that could be used for developing continuum mechanics-based material models.
- Fatigue damage models can be derived by using the data since information regarding the cycles to failure, stiffness degradation curves and hysteresis loops for different applied stress levels is provided.
- Comparisons to available literature data can assist matrial selection procedures for wind turbine rotor blade assembly.
- The wind turbine adhesively bonded joint behavior can be assessed in the frame of stress-life based approaches by utilizing the data.

2. Data Description

This article describes the raw, processed, and analyzed data on the effect of adhesive specimen geometry and toughening effect on the fatigue life of wind turbine blade adhesives. Herein, the data collection process and experimental data of each specimen of different adhesive materials groups are presented whereas the conclusive results are found in [1]. The plots from Figs. 1-17 can be replicated using the published Zenodo data [2]. Table 1 provides the figure and table captions and their associated data file. ‘X’ means the corresponding specimen name.

Table 1
Guidelines for referring the data files.

S.No	Table/Figure no	Zenedo data file	Folder name
1	Fig. 1	X.xlsx	01_Static.zip
2	Fig. 2	X.xlsx	01_Static.zip
3	Figs. 3–5	X.xlsx	02_Hysteresis.zip
4	Figs. 6–11	X.xlsx	03_Fatigue.zip
5	Figs. 12–17	X.xlsx	03_Fatigue.zip
6	Raw data for Figs. 6–17	TST_2022-04_FA_###.csv	04_Fatigue_Rawdata.zip
7	Fig. 19	05_Fatigue_analysis.mlx	-

2.1. Uniaxial Tensile Data

The tensile properties of the pristine and hybrid adhesives at standardized strain rate (Tables 2-5) and high strain rate (Tables 6-9) are provided in this subsection.

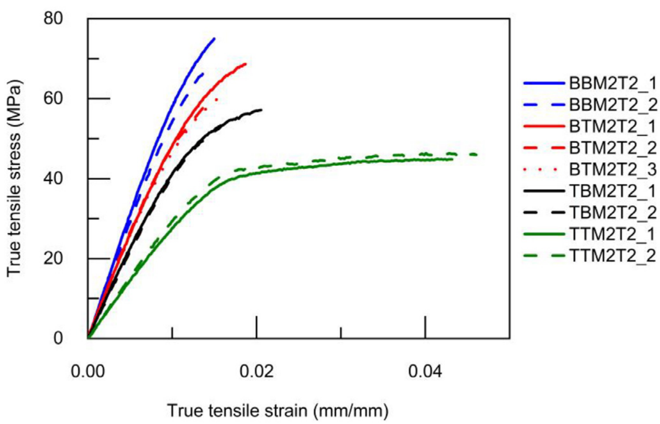

Fig. 1. True stress versus true strain of adhesives at standardized strain rate.

Table 2
Tensile properties of non-toughened epoxy BBM2T2 at standardized strain rate.

Property	Unit	BBM2T2		
		S1	S2	Average
Young's modulus, E	GPa	6.18	5.63	5.90 ± 0.27
Maximum stress, σ_u	MPa	74.94	67.92	71.43 ± 3.51
Strain at failure, ε_f	mm/mm	0.015	0.0143	0.0146 ± 0.0003
Tensile toughness, U_T	KJ/m^3	0.638	0.555	0.596±0.042

Table 3
Tensile properties of hybrid epoxy BTM2T2 at standardized strain rate.

Property	Unit	BTM2T2			
		S1	S2	S3	Average
Young's modulus, E	GPa	5.07	4.99	4.74	4.93 ± 0.14
Maximum stress, σ_u	MPa	68.65	57.91	60.54	62.37 ± 4.57
Strain at failure, ε_f	mm/mm	0.0187	0.0137	0.0154	0.0159 ± 0.0021
Tensile toughness, U_T	KJ/m^3	0.779	0.456	0.541	0.592±0.137

Table 4
Tensile properties of hybrid epoxy TBM2T2 at standardized strain rate.

Property	Unit	TBM2T2		
		S1	S2	Average
Young's modulus, E	GPa	4.35	4.26	4.30 ± 0.04
Maximum stress, σ_u	MPa	57.17	53.09	55.13 ± 2.04
Strain at failure, ε_f	mm/mm	0.0205	0.0158	0.0181 ± 0.0023
Tensile toughness, U_T	KJ/m^3	0.761	0.489	0.625±0.136

Table 5
Tensile properties of toughened epoxy TTM2T2 at standardized strain rate.

Property	Unit	TTM2T2		
		S1	S2	Average
Young's modulus, E	GPa	2.78	2.975	2.88 ± 0.10
Maximum stress, σ_u	MPa	44.96	46.37	44.47 ± 1.26
Strain at failure, ε_f	mm/mm	0.0415	0.0429	0.0417 ± 0.0054
Tensile toughness, U_T	KJ/m^3	1.518	1.706	1.612±0.094

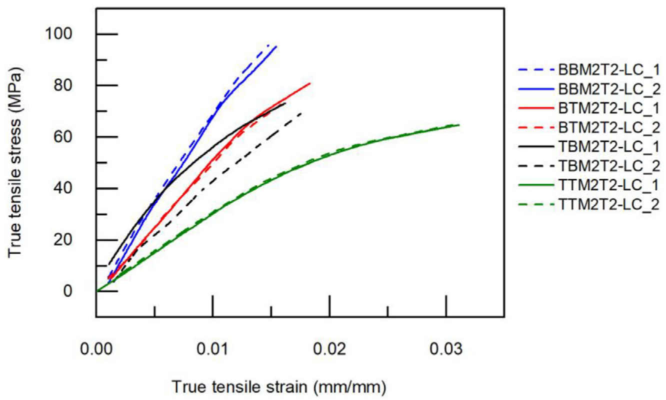

Fig. 2. True stress versus true strain of adhesives at high strain rate.

Table 6
Tensile properties of non-toughened epoxy BBM2T2 at high strain rate.

Property	Unit	BBM2T2-LC		
		S1	S2	Average
Young's modulus, E	GPa	6.91	6.88	6.895 ± 0.015
Maximum stress, σ_u	MPa	95.23	95.76	95.495 ± 0.265
Strain at failure, ε_f	mm/mm	0.0154	0.0148	0.0151 ± 0.0003
Tensile toughness, U_T	KJ/m^3	0.775	0.746	0.761±0.015

Table 7
Tensile properties of non-toughened epoxy BTM2T2 at high strain rate.

Property	Unit	BTM2T2-LC		
		S1	S2	Average
Young's modulus, E	GPa	5.25	5.05	5.15 ± 0.1
Maximum stress, σ_u	MPa	80.88	72.71	76.795 ± 4.085
Strain at failure, ε_f	mm/mm	0.0183	0.0158	0.01705 ± 0.00125
Tensile toughness, U_T	KJ/m^3	0.790	0.611	0.700±0.089

Table 8
Tensile properties of non-toughened epoxy TBM2T2 at high strain rate.

Property	Unit	TBM2T2-LC		
		S1	S2	Average
Young's modulus, E	GPa	4.27	3.95	4.11 ± 0.16
Maximum stress, σ_u	MPa	73.24	69.17	71.205 ± 2.035
Strain at failure, ε_f	mm/mm	0.0162	0.0175	0.01685 ± 0.00065
Tensile toughness, U_T	KJ/m^3	0.730	0.634	0.682±0.048

Table 9
Tensile properties of non-toughened epoxy TTM2T2 at high strain rate.

Property	Unit	TTM2T2-LC		
		S1	S2	Average
Young's modulus, E	GPa	2.94	2.891	2.9155 ± 0.0245
Maximum stress, σ_u	MPa	64.77	64.79	64.78 ± 0.01
Strain at failure, ε_f	mm/mm	0.0306	0.0311	0.03085 ± 0.00025
Tensile toughness, U_T	KJ/m^3	1.218	1.240	1.229±0.011

2.2. Tensile-Tensile Fatigue Data

2.2.1. Hysteresis Loops

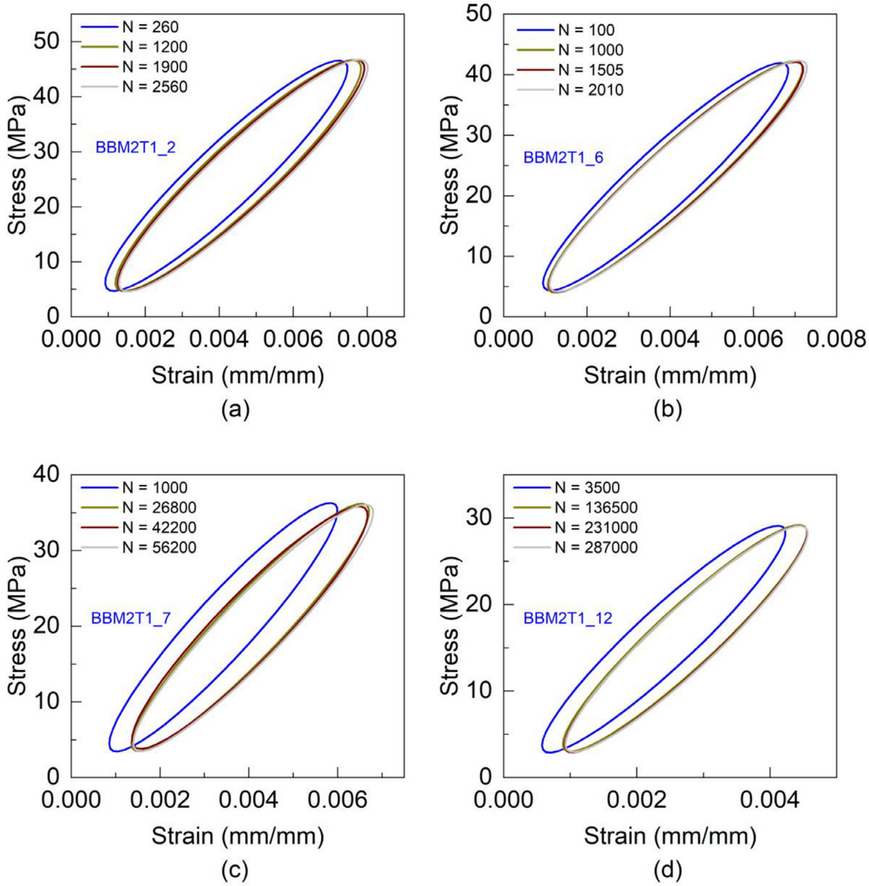

Fig. 3. Hysteresis loops of non-toughened, Type I adhesive (a) BBM2T1_2, (b) BBM2T1_6, (c) BBM2T1_7 and (d) BBM2T1_12.

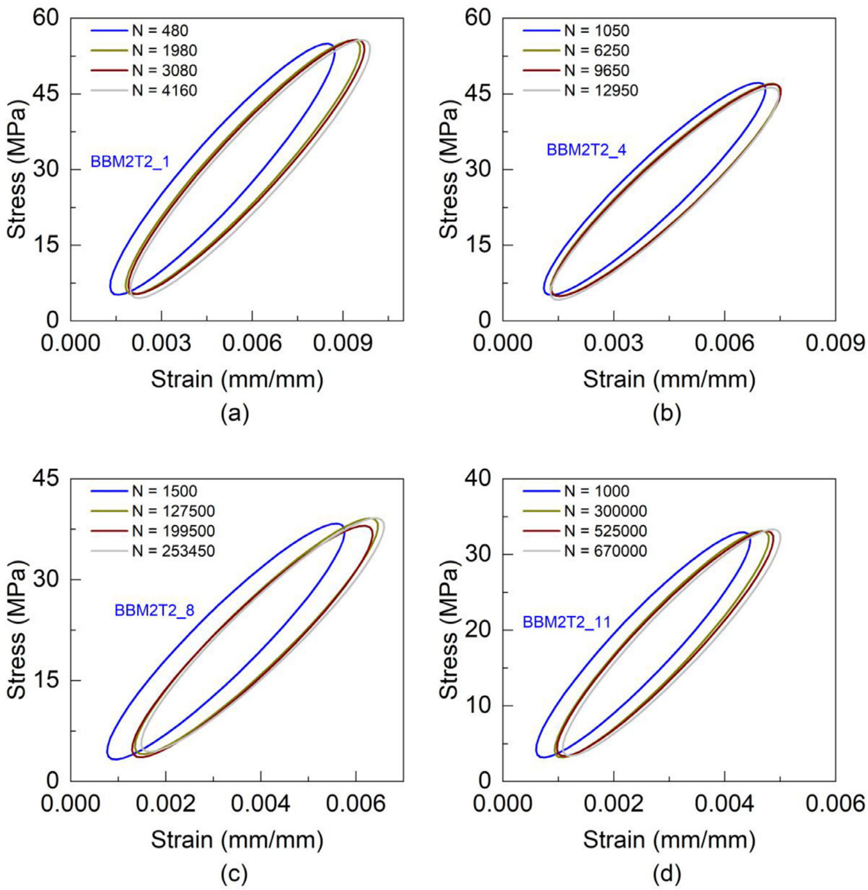

Fig. 4. Hysteresis loops of non-toughened, Type II adhesive (a) BBM2T2_1, (b) BBM2T2_4, (c) BBM2T2_8 and (d) BBM2T2_11.

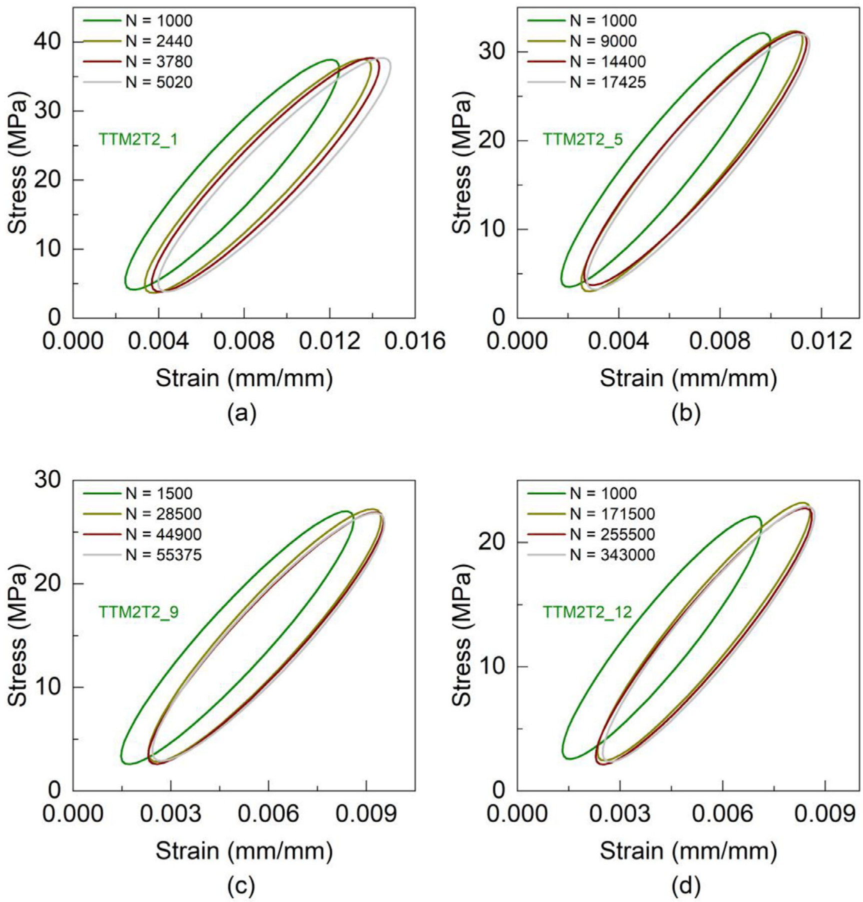

Fig. 5. Hysteresis loops of toughened, Type II adhesive (a) TTM2T2_1, (b) TTM2T2_5, (c) TTM2T2_9 and (d) TTM2T2_12.

2.2.2. Mean Strain Evolution Plots

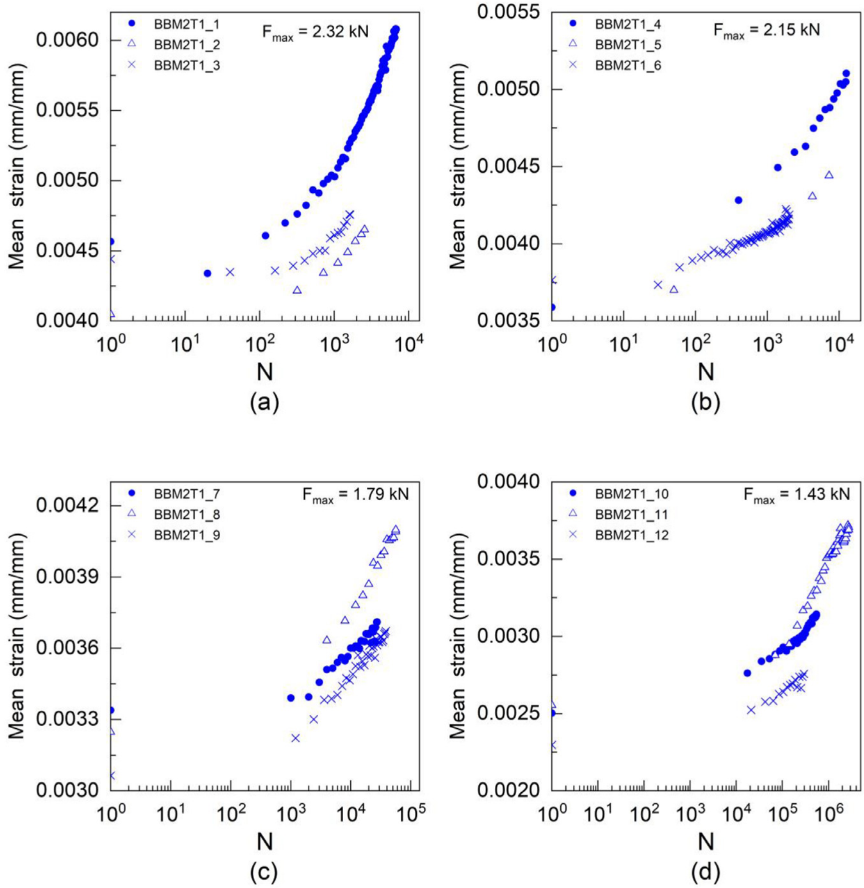

Fig. 6. Normalized stiffness versus normalized cycle response of non-toughened, Type I, pristine adhesive (BBM2T1) (a) at 2.32 kN (b) at 2.15 kN, (c) at 1.79 kN and (d) at 1.43 kN.

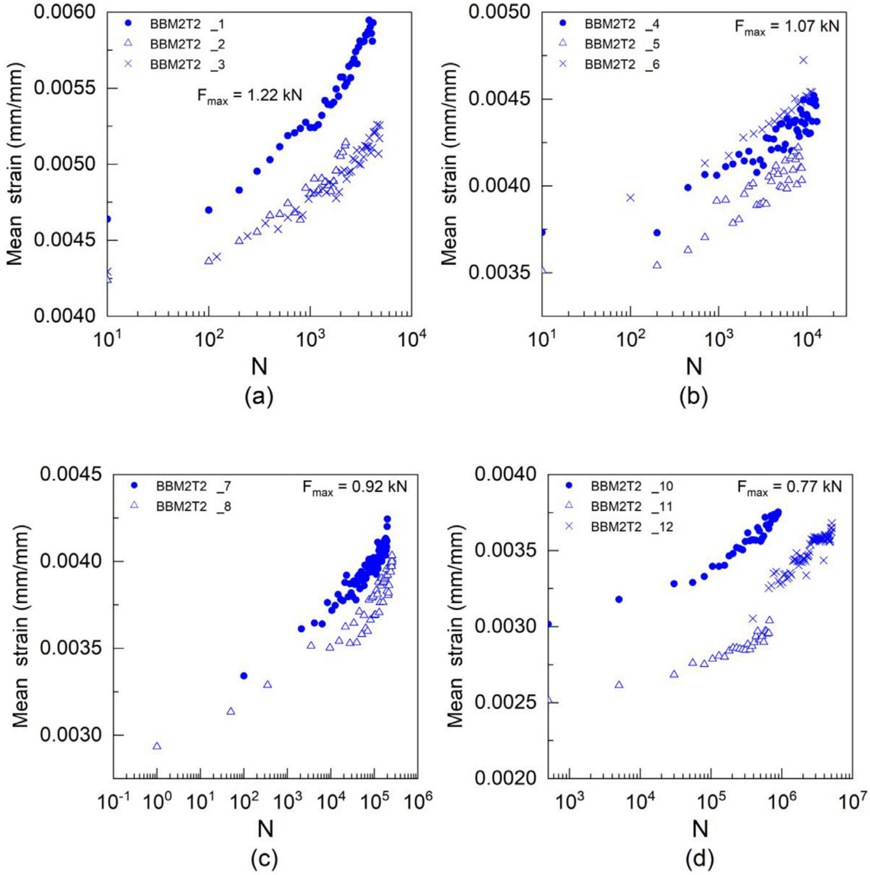

Fig. 7. Normalized stiffness versus normalized cycle response of non-toughened, Type II, pristine adhesive (BBM2T2) (a) at 1.22 kN (b) at 1.07 kN, (c) at 0.92 kN and (d) at 0.77 kN.

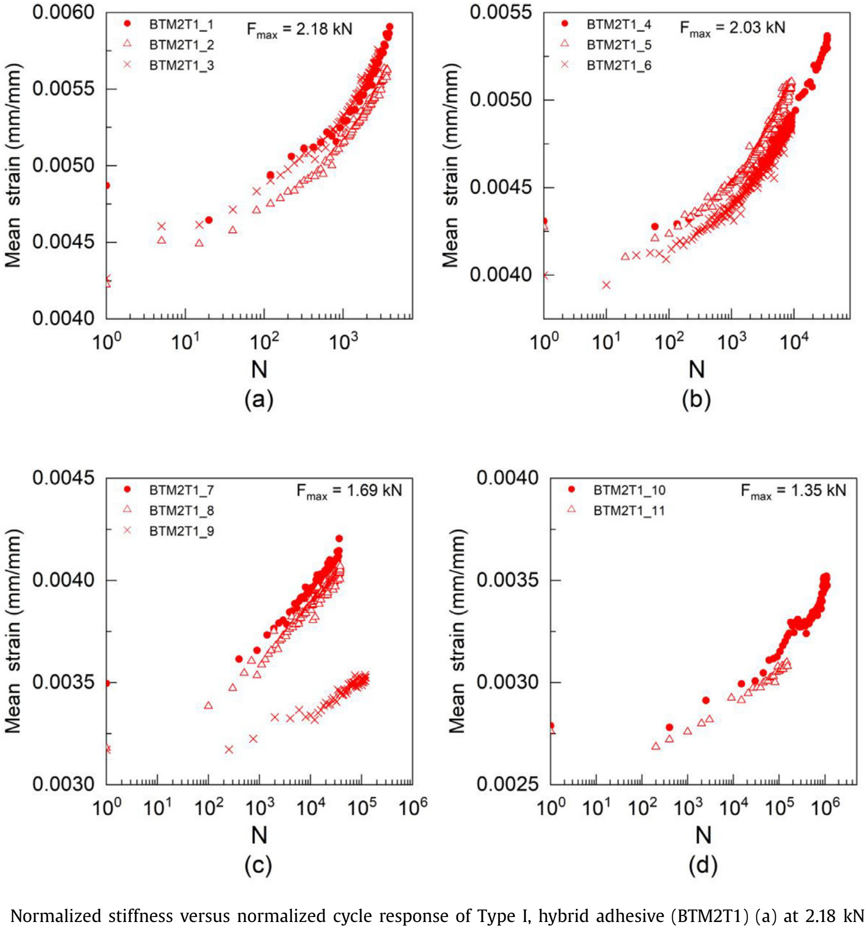

Fig. 8. Normalized stiffness versus normalized cycle response of Type I, hybrid adhesive (BTM2T1) (a) at 2.18 kN (b) at 2.03 kN, (c) at 1.69 kN and (d) at 1.35 kN.

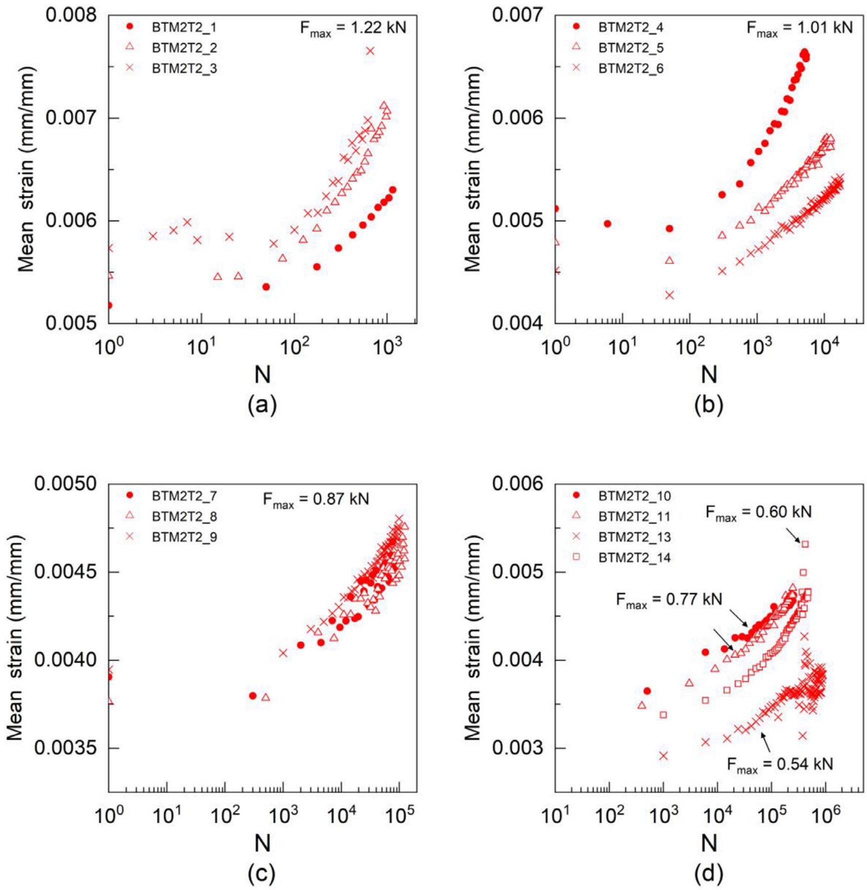

Fig. 9. Normalized stiffness versus normalized cycle response of Type II, hybrid adhesive (BTM2T2) (a) at 1.22 kN (b) at 1.01 kN, (c) at 0.87 kN and (d) at 0.77, 0.60 & 0.54 kN.

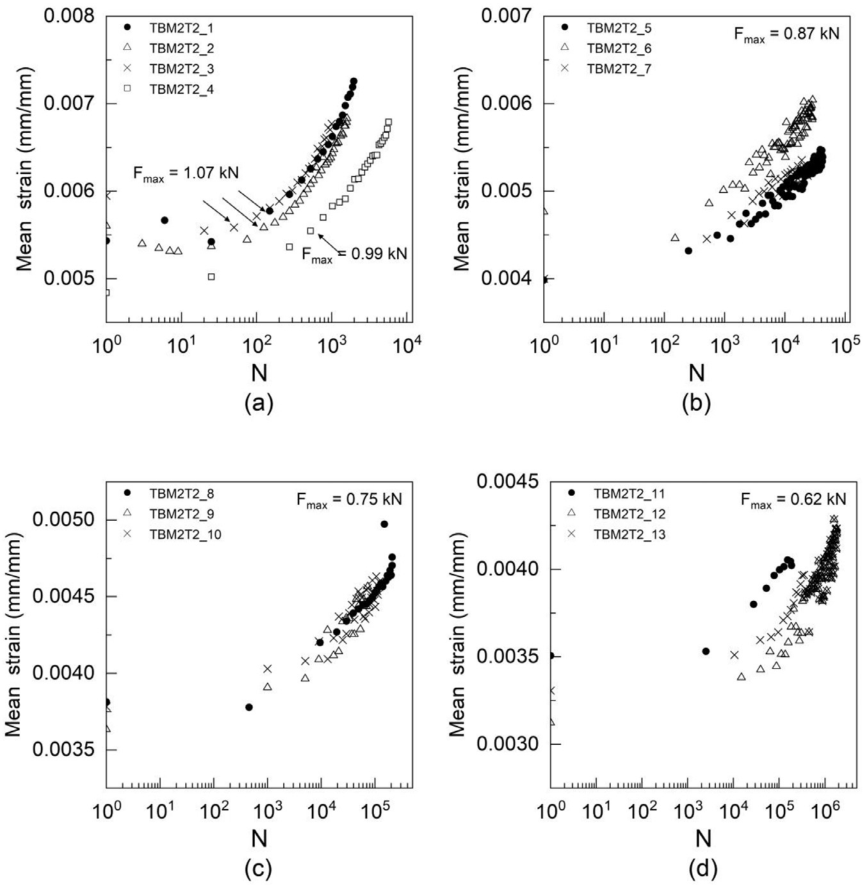

Fig. 10. Normalized stiffness versus normalized cycle response of Type II, hybrid adhesive (TBM2T2) (a) at 1.07 & 0.99 kN (b) at 0.87 kN, (c) at 0.75 kN and (d) at 0.62 kN.

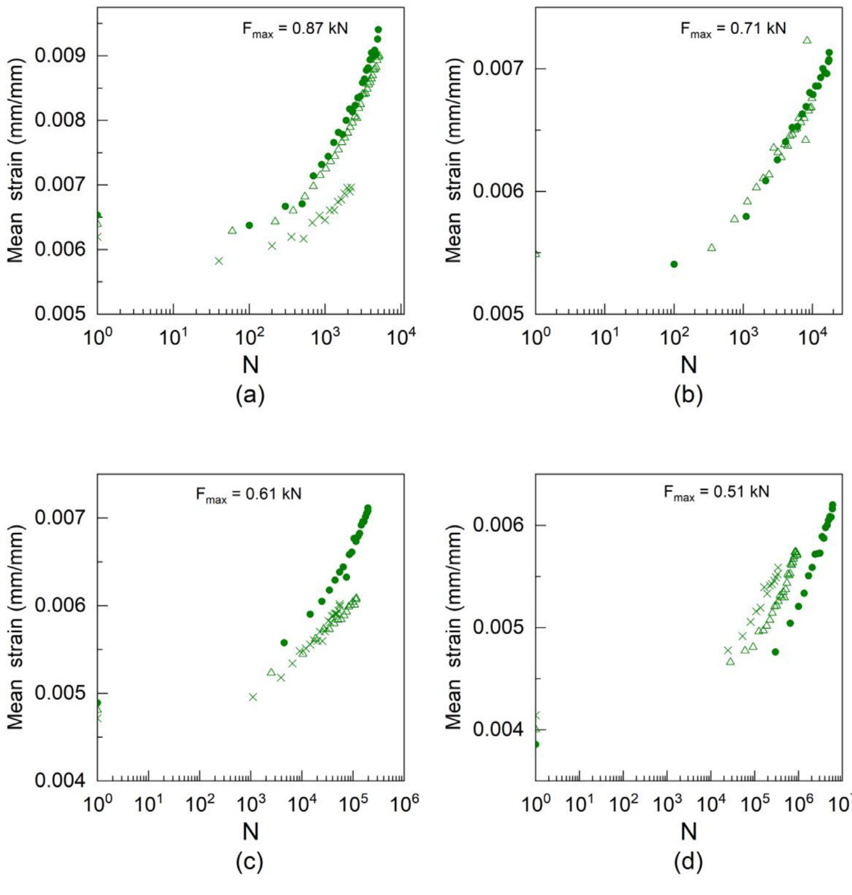

Fig. 11. Normalized stiffness versus normalized cycle response of toughened, Type II, pristine adhesive (TTM2T2) (a) at 0.82 kN (b) at 0.71 kN, (c) at 0.61 kN and (d) at 0.51 kN

2.2.3. Stiffness Degradation Plots

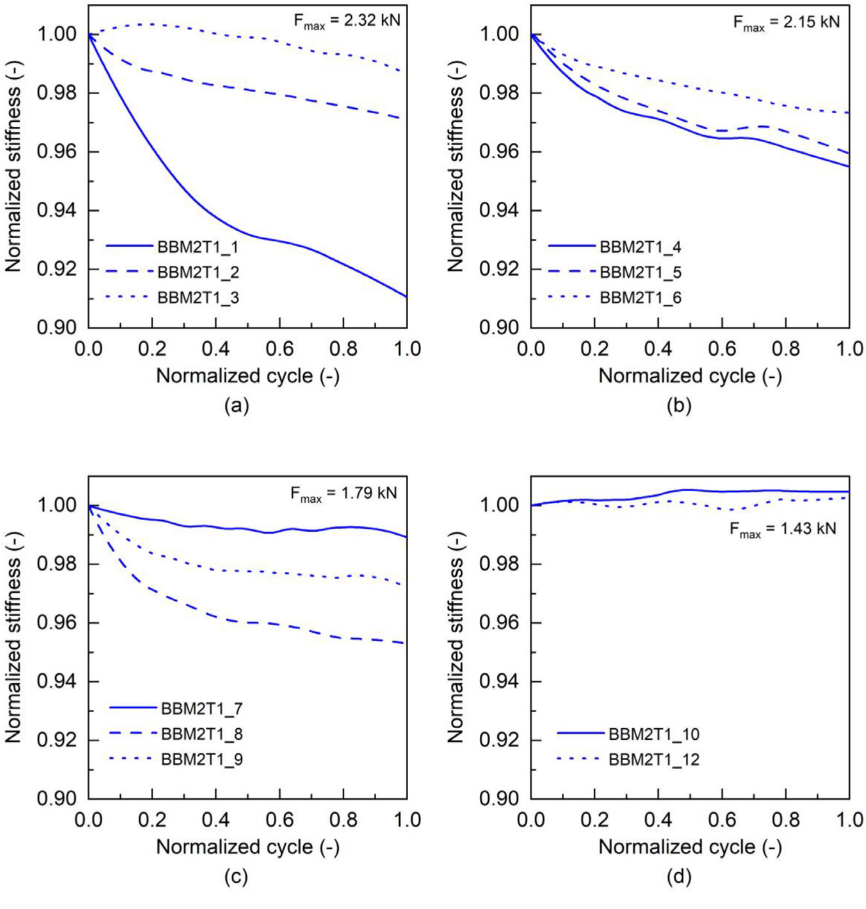

Fig. 12. Normalized stiffness versus normalized cycle response of non-toughened, Type I, pristine adhesive (BBM2T1) (a) at 2.32 kN (b) at 2.15 kN, (c) at 1.79 kN and (d) at 1.43 kN.

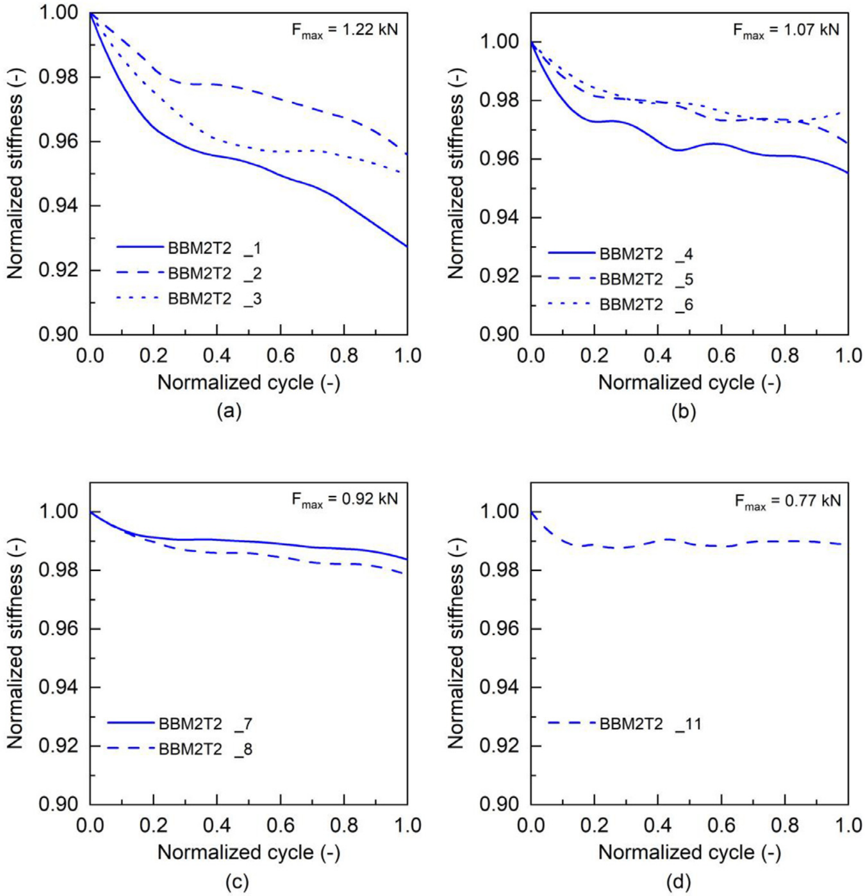

Fig. 13. Normalized stiffness versus normalized cycle response of non-toughened, Type II, pristine adhesive (BBM2T2) (a) at 1.22 kN (b) at 1.07 kN, (c) at 0.92 kN and (d) at 0.77 kN.

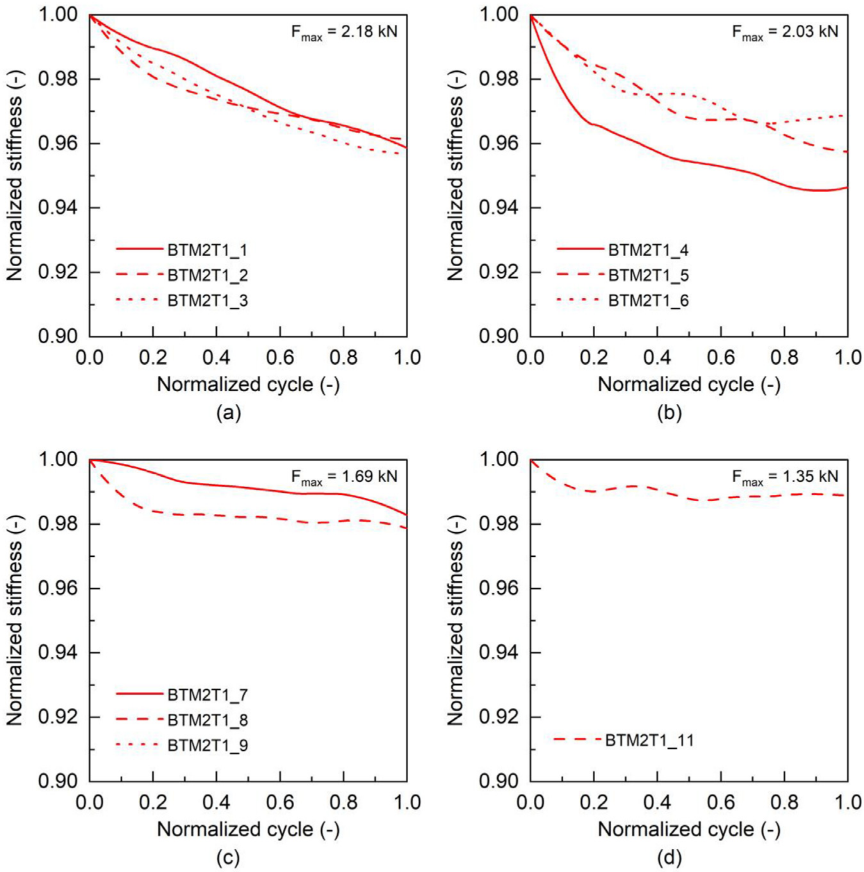

Fig. 14. Normalized stiffness versus normalized cycle response of Type I, hybrid adhesive (BTM2T1) (a) at 2.18 kN (b) at 2.03 kN, (c) at 1.69 kN and (d) at 1.35 kN.

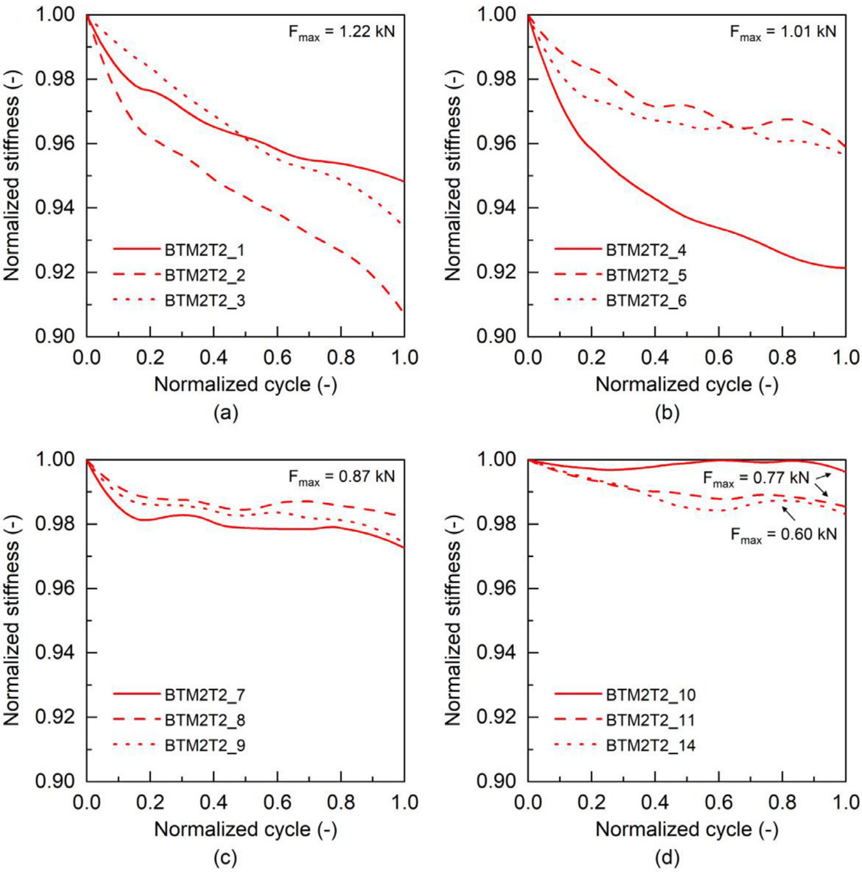

Fig. 15. Normalized stiffness versus normalized cycle response of Type II, hybrid adhesive (BTM2T2) (a) at 1.22 kN (b) at 1.01 kN, (c) at 0.87 kN and (d) at 0.77 & 0.60 kN.

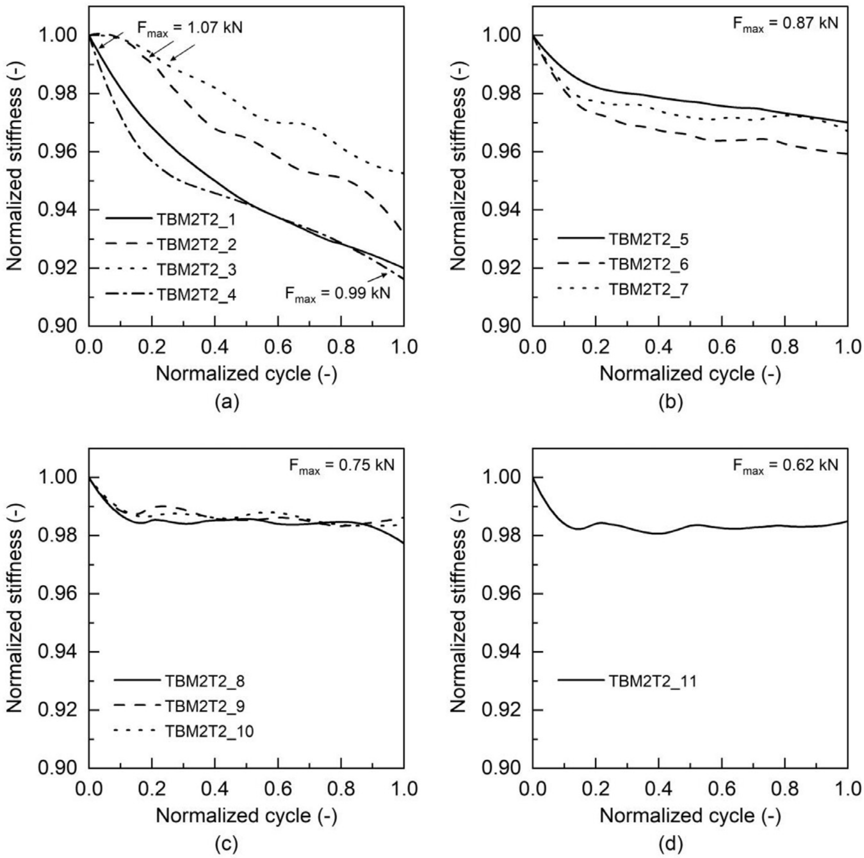

Fig. 16. Normalized stiffness versus normalized cycle response of Type II, hybrid adhesive (TBM2T2) (a) at 1.07 & 0.99 kN (b) at 0.87 kN, (c) at 0.75 kN and (d) at 0.62 kN.

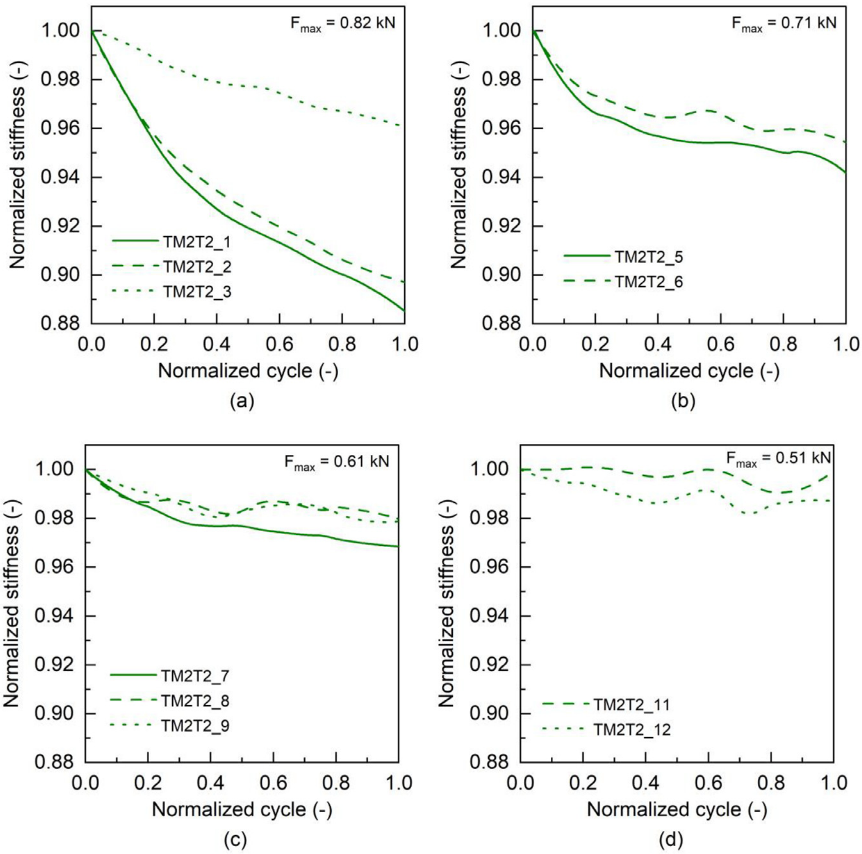

Fig. 17. Normalized stiffness versus normalized cycle response of toughened, Type II, pristine adhesive (TTM2T2) (a) at 0.82 kN (b) at 0.71 kN, (c) at 0.61 kN and (d) at 0.51 kN.

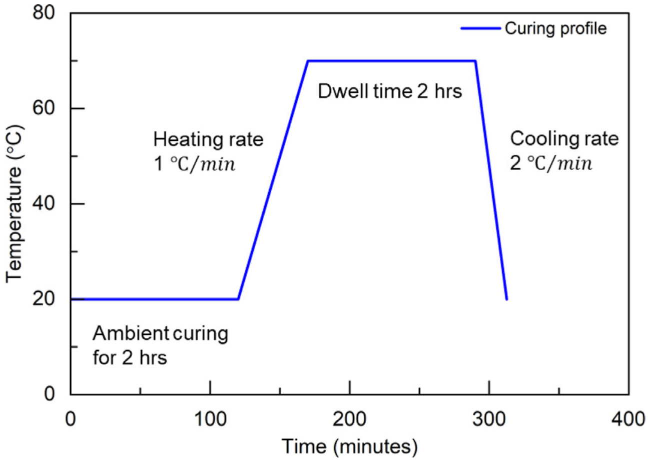

Fig. 18. Curing profile of the epoxy adhesives [3].

3. Experimental Design, Materials and Methods

3.1. Materials

SPABOND™ 820HTA (non-toughened) and SPABOND™ 840HTA (toughened) adhesives were used to fabricate the pristine and hybrid through manual mixing technique M2. The pristine and hybrid adhesive compositions are mentioned in Table 10. SP refers to Spabond adhesive.

Table 10
Adhesive material composition.

Adhesive	Base	Hardener	Comments
BBM2	SP 820	SP 820	pristine, non-toughened
BTM2	SP 820 + SP 840	SP 820 + SP 840	hybrid, 75:25 wt%
TBM2	SP 820 + SP 840	SP 820 + SP 840	hybrid, 50:50 wt%
TTM2	SP 840	SP 840	pristine, toughened

3.2. Manufacturing

The epoxy adhesive base and hardener material were weighed at a ratio of 100:33 and they were manually mixed using a wooden spatula for 5–7 min. The adhesive material was degassed for 7 min, under a vacuum pressure of 0.95 bar to eliminate the entrapped air due to the mixing process. Nonetheless, the high viscosity of the adhesive material made it challenging to remove all air bubbles completely. An aluminum plate with sidebars of 4 mm thickness was coated twice with a mold release agent, Sika® liquid wax-815, using a brush, and left to dry for 15 ± 5 min at an ambient temperature of 20 °C ± 2 °C. The mixed adhesive was then applied inside the mold cavity with care using an adhesive spreader, and any excess material was removed using a scraper. Fig. 18 shows the curing cycle of the epoxy adhesives that was maintained by the forced convection oven, Memmert® [3].

Following the curing procedure, the Type I and Type II specimens were cut to the required dimensions using a water-jet cutting machine.

3.3. Experimental Methods

The uniaxial tensile and fatigue experimental setup and parameters are provided in Tables 11-13. The force values from the test machine and the corresponding images from the camera were collected by the DAQ software (Fig. 19). Further, the images were analyzed by VIC2D 6 software to determine the engineering strain. The strain values were matched with the recorded load values. Further, the static and fatigue properties were analyzed with Matlab R2021b® software. A Matlab program file to calculate the cyclic stress and strains, construct hysteresis loops, calculate the mean strain evolution and derive the stiffness degradation plots (05_Fatigue_analysis.mlx) is provided with this article. The raw data files (TST_2022-04_FA_###.csv) and the metadata file (TST_2022-04_FA_metadata.xlsx) were created according to the CCFATIGUE data convention (https://ccfatigue-test.epfl.ch/fatigue_database/search).

Table 11
Uniaxial tensile at standardized strain rate experimental setup and parameters.

Testing parameters	Comment
Nominal dimension	Refer to ASTM D638-22 Type II dog-bone specimen
Test equipment	MTS® 810 Landmark servo-hydraulic machine
Load cell capacity	Calibrated for 5 kN with an accuracy of ±0.2%.
Displacement rate	1 mm/min
Strain measurement	DIC technique
Camera	Point Grey – Grasshopper 3 camera (2.2 Megapixels) housing Fujinon HF35SA-1 35 mm F/1.4 lens.
DIC analysis software	VIC2D 6
ASTM standard	ASTM D638-14
DAQ software	Labview®

Table 12
Uniaxial tensile at high strain rate experimental setup and parameters.

Testing parameters	Comment
Nominal dimension	Refer to ASTM D638-22 Type II dog-bone specimen
Test equipment	MTS® 810 Landmark servo-hydraulic machine
Load cell capacity	Calibrated for 5 kN with an accuracy of ±0.2%.
Force rate	11.9 kN/s and 17.9 kN/s
Strain measurement	DIC technique
Camera	FASTCAM SA- Z from Photron along with AF-S NIKKOR 50 mm lens
DIC analysis software	VIC2D 6
ASTM standard	ASTM D638-14
DAQ software	Catman®

Table 13
Tensile-tensile fatigue experimental setup and parameters.

Testing parameters	Comment
Nominal dimension	Refer to ASTM D638-22 Type I and Type II dog-bone specimen
Test equipment	MTS® 810 Landmark servo-hydraulic machine
Load cell capacity	Calibrated for 5 kN with an accuracy of ±0.2%.
Displacement rate	1 mm/min until reaching the mean load
Cyclic frequency	10 Hz
Stress ratio	0.1
Strain measurement	DIC technique
Camera	Point Grey – Grasshopper 3 camera (2.2 Megapixels) housing Fujinon HF35SA-1 35 mm F/1.4 lens.
DIC analysis software	VIC2D 6
ASTM standard	ASTM D638-14
DAQ software	Labview®

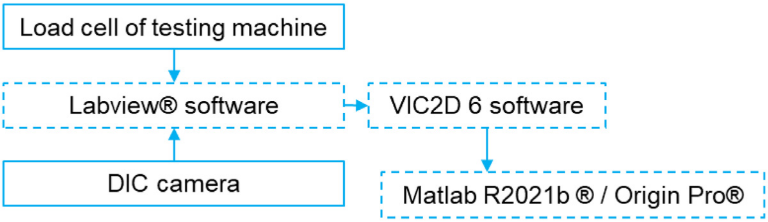

Fig. 19. DIC data collection in static and fatigue experiments [3].

Ethics Statement

This work did not involve human subjects, animal experiments, or data collected from social media platforms.

Data Availability

Fatigue dataset of hybrid non-toughened and toughened epoxy adhesives (Original data) (ZENODO).

CRediT Author Statement

Dharun Vadugappatty Srinivasan: Conceptualization, Methodology, Data curation, Writing – original draft, Investigation; **Anastasios P. Vassilopoulos:** Conceptualization, Supervision, Validation, Writing – review & editing, Funding acquisition.

Acknowledgments

The authors wish to acknowledge the support and funding of this research by the Swiss National Science Foundation (Grant No. IZCOZ0_189905) under the project, Bonded composite primary structures in engineering applications (BONDS), the assistance provided by the technical team of the structural engineering experimental platform (GIS-ENAC) at the Ecole Polytechnique Fédérale de Lausanne (EPFL), Switzerland and Gurit UK Ltd for providing the adhesive materials and for many helpful discussions. This article/publication is based upon work from COST Action CA18120 (CERTBOND - https://certbond.eu/), supported by COST (European Cooperation in Science and Technology).

Declaration of Competing Interest

The authors declare that they have no known competing financial interests or personal relationships that could have appeared to influence the work reported in this paper.

References

[1] D.V. Srinivasan, A.P. Vassilopoulos, Fatigue performance of wind turbine rotor blade epoxy adhesives, Polym Test. 121 (2023) 107975, doi:10.1016/J.POLYMERTESTING.2023.107975.
[2] D.V. Srinivasan, A.P. Vassilopoulos, Fatigue properties of wind turbine rotor blade hybrid epoxy adhesives, (2023). https://doi.org/10.5281/zenodo.7974627.
[3] D.V. Srinivasan, A.P. Vassilopoulos, Dataset for the hybrid non-toughened and toughened epoxy adhesive properties, Data Brief 47 (2023) 108912, doi:10.1016/J.DIB.2023.108912.